Competition between Antiferromagnetic and Superconducting States, Electron-Hole Doping Asymmetry, and Fermi-Surface Topology in High Temperature Superconductors

Sandeep Pathak,[1] Vijay B. Shenoy,[2,1] Mohit Randeria,[3] and Nandini Trivedi[3]
[1]*Materials Research Centre, Indian Institute of Science, Bangalore 560 012, India*
[2]*Centre for Condensed Matter Theory, Indian Institute of Science, Bangalore 560 012, India*
[3]*Physics Department, Ohio State University, 191 W Woodruff Avenue, Columbus, Ohio 43210, USA*
(Received 19 June 2008; published 13 January 2009)

We investigate the asymmetry between electron and hole doping in a 2D Mott insulator and the resulting competition between antiferromagnetism (AFM) and *d*-wave superconductivity (SC), using variational Monte Carlo calculations for projected wave functions. We find that key features of the $T = 0$ phase diagram, such as critical doping for SC-AFM coexistence and the maximum value of the SC order parameter, are determined by a single parameter η which characterizes the topology of the "Fermi surface" at half filling defined by the bare tight-binding parameters. Our results give insight into why AFM wins for electron doping, while SC is dominant on the hole-doped side. We also suggest using band structure engineering to control the η parameter for enhancing SC.

DOI: 10.1103/PhysRevLett.102.027002 PACS numbers: 74.72.−h, 74.20.−z, 74.25.Dw, 75.10.Jm

Ever since their discovery, cuprates have continued to pose some of the most challenging puzzles [1–3] in condensed matter physics. Cuprate phase diagrams exhibit an antiferromagnetic ground state for undoped or low doped compounds giving way to a superconducting ground state at higher doping. A notable aspect of the experimental phase diagram is the "electron-hole" asymmetry [4]; i.e., antiferromagnetism (AFM) survives to a much higher doping on the electron-doped side, while superconductivity (SC) is "stronger" on the hole-doped side. In this Letter we address the following outstanding questions about the phase diagram: What controls the electron-hole asymmetry in cuprates? How can we understand the material dependence, e.g., empirical correlation between electronic structure parameters—the range of the in-plane hopping—and SC, pointed out by Pavarini *et al.* [5]? In particular, can we get some insight into the all important question of what material parameters control the optimal SC transition temperature $T_c^{\max}$?

The essential strong correlation physics of high T_c superconductivity is well described by the *t-J* model and its variants [4,6–9]. Ground state studies, based on the variational Monte Carlo method which treats the "no-double occupancy" constraint exactly, have been inspired by Anderson's idea of resonating valance bond (RVB) state [6]. Previous studies [10–12] investigated the competition between AFM and SC. However, a unified understanding of the questions raised above has yet to emerge.

Here we show that, rather surprisingly, a single parameter η, which characterizes the topology of the "Fermi surface" at half filling, determines the key features of the phase diagram, thereby providing a resolution to the questions raised above. Furthermore, our results directly indicate a route to enhancing the optimal superconducting transition temperature by band structure engineering.

Model.—The minimal model that allows for an understanding of the material dependencies of the cuprate phenomenology is the *t-J* model with extended hopping: $\mathcal{H} = -P\sum_{i,j,\sigma} t_{i,j}(c^\dagger_{i\sigma}c_{j\sigma} + \text{H.c.})P + J\sum_{\langle i,j\rangle}(\boldsymbol{S}_i \cdot \boldsymbol{S}_j - n_i n_j/4)$, where $c_{i\sigma}$ is the electron operator at site i with spin σ, $n_{i\sigma} = c^\dagger_{i\sigma}c_{i\sigma}$ is the density with $n_i = \sum_\sigma n_{i\sigma}$, $\boldsymbol{S}_i = \frac{1}{2}c^\dagger_{i\alpha}\vec{\sigma}_{\alpha\beta}c_{i\beta}$ is the spin at site i (σ's are the Pauli matrices), and J is the antiferromagnetic exchange between nearest neighbors $\langle i, j\rangle$. The projection operator $P = \prod_i(1 - n_{i\uparrow}n_{i\downarrow})$ implements the no-double occupancy constraint.

The bare dispersion has the form $\epsilon(\mathbf{k}) = -2t(\cos k_x + \cos k_y) + 4t' \cos k_x \cos k_y - 2t''(\cos 2k_x + \cos 2k_y)$, where t, t', and t'' are the nearest-, second-, and third-neighbor hoppings, respectively. The importance of t' and t'' is suggested both by angle-resolved photoemission spectroscopy experiments [13] and electronic structure calculations [14]. With the sign convention above, t, t', and t'' are all positive for the hole-doped case. To model the electron-doped case, we make a standard particle-hole transformation $\tilde{c}_{i\sigma} = (-1)^i c_{i\sigma}$ in $\mathcal{H}$. Thus for the electron-doped case, we again obtain $\mathcal{H}$ with $\tilde{t} = t$, $\tilde{t'} = -t'$, and $\tilde{t''} = -t''$.

Variational wave function.—We choose a variational ground state wave function for an N-particle system that includes both AFM and SC order:

$$|\Psi_0\rangle = P\left[\sum_{ij}\varphi(\mathbf{r}_i - \mathbf{r}_j)c^\dagger_{i\uparrow}c^\dagger_{j\downarrow}\right]^{N/2}|0\rangle. \tag{1}$$

The form of φ in the unprojected wave function is motivated by a saddle point analysis of $\mathcal{H}$. For a nonzero Néel amplitude m_N, we get two spin density wave bands ($\alpha = 1,\ 2$): $E_{(1,2)}(\mathbf{k}) = [\xi(\mathbf{k}) + \xi(\mathbf{k} + \boldsymbol{Q})]/2 \pm (1/2) \times \sqrt{[\xi(\mathbf{k}) - \xi(\mathbf{k} + \boldsymbol{Q})]^2 + 16J^2m_N^2}$, where $\boldsymbol{Q} = (\pi, \pi)$

and $\xi(\mathbf{k}) = -2t(\cos k_x + \cos k_y) + 4t'_{\rm var}\cos k_x \cos k_y - 2t''_{\rm var}(\cos 2k_x + \cos 2k_y) - \mu_{\rm var}$, with $\mathbf{k}$ in the reduced Brillouin zone. The d-wave pairing field $\Delta(\mathbf{k}) = J\Delta(\cos k_x - \cos k_y)$ gives rise to SC in the two spin density wave bands, with BCS coherence factors

$$\frac{v_{\mathbf{k}\alpha}}{u_{\mathbf{k}\alpha}} = (-1)^{\alpha-1}\frac{\Delta(\mathbf{k})}{E_\alpha(\mathbf{k}) + \sqrt{E_\alpha^2(\mathbf{k}) + \Delta^2(\mathbf{k})}}. \quad (2)$$

The internal pair wave function $\varphi(\mathbf{r}_i - \mathbf{r}_j)$ is given by the Fourier transforming $v_{\mathbf{k}\alpha}/u_{\mathbf{k}\alpha}$ and by summing over the two spin density wave bands α. At half filling the $tt't''J$ model is simply the nearest-neighbor Heisenberg model (independent of t', t''), whose Néel order motivates the choice of $\boldsymbol{Q} = (\pi, \pi)$, quite unrelated to nesting physics. For simplicity we choose $\boldsymbol{Q}$ to be doping independent following Refs. [10–12]. Our wave function generalizes that of Ref. [11] to include the variational Fock shifts $t'_{\rm var}$ and $t''_{\rm var}$.

The five variational parameters in $|\Psi_0\rangle$ are the Néel amplitude m_N, the d-wave gap Δ, the (Hartree-shifted) chemical potential $\mu_{\rm var}$, and $t'_{\rm var}$ and $t''_{\rm var}$ renormalized by Fock shifts. Their optimum values are determined by minimizing the ground state energy $E = \langle\Psi_0|\mathcal{H}|\Psi_0\rangle/\langle\Psi_0|\Psi_0\rangle$ calculated using variational Monte Carlo (VMC) calculations, which exactly implements the projection P. We have developed a fast conjugate gradient algorithm (details will be published elsewhere) that evaluates derivatives of the energy and efficiently determines the optimized variational parameters.

Results.—The $T = 0$ phase diagram is determined by computing the SC and AFM order parameters for the optimized ground state as a function of doping [15]. The SC order parameter [7] $\Phi = \lim_{|\boldsymbol{r}-\boldsymbol{r}'|\to\infty} F_{\alpha,\alpha}(\boldsymbol{r} - \boldsymbol{r}')$ is obtained from the long range behavior of the correlation function $F_{\alpha,\beta}(\boldsymbol{r} - \boldsymbol{r}') = \langle B^\dagger_{r\alpha} B_{r'\beta}\rangle$, where $B^\dagger_{r\alpha} = \frac{1}{2}\times(c^\dagger_{\boldsymbol{r}\uparrow}c^\dagger_{\boldsymbol{r}+\hat{\alpha}\downarrow} - c^\dagger_{\boldsymbol{r}\downarrow}c^\dagger_{\boldsymbol{r}+\hat{\alpha}\uparrow})$ creates a singlet on the bond $(\boldsymbol{r}, \boldsymbol{r} + \hat{\alpha})$, $\alpha = x, y$. The AFM order parameter $M = (2/N)\times\langle\sum_{i\in A} S^z_i - \sum_{i\in B} S^z_i\rangle$ is the difference of the magnetization on the A and B sublattices.

In Fig. 1 we see the following phases: an AFM Mott insulator at half filling; coexistence of SC and AFM for small (electron-hole) doping; a d-wave SC at higher doping; and a Fermi liquid for sufficiently large doping. The phase diagram shows marked electron-hole asymmetry for $t' \neq 0$. As the next-neighbor hopping $|t'|$ increases, SC is enhanced on the hole-doped side, while AFM is stabilized on the electron-doped side. These results are consistent with earlier VMC calculations [7,8,10–12,16] and dynamical mean-field studies [17,18].

Our new findings are that, on the hole-doped side, $|t'|$ does not affect AFM, and, in particular, the critical doping $x_{\rm AFM}$, beyond which AFM vanishes, is insensitive to the value of $|t'|$. On the electron-doped side, SC is slightly weakened and the peak value of the SC order parameter $\Phi_{\rm max}$ falls with increasing $|t'|$.

Upon adding a second-neighbor hopping t'', we find the following general trends: (a) On the hole-doped side, an increase in t'' leads to an increase of superconducting correlations. Interestingly, AFM is relatively unaffected, and $x_{\rm AFM}$ is quite insensitive to t''. (b) On the electron-doped side, AFM is enhanced with increasing $|t''|$, and superconductivity is essentially unaffected. We have also performed calculations using a simple renormalized mean-field theory [8,19], and the qualitative phase diagram is in agreement with the VMC results.

At very low doping, our results differ from experiments due to the neglect of long range Coulomb and disorder effects. Once the local superfluid density becomes sufficiently small near half filling due to projection [7], the long-wavelength, quantum phase fluctuations that were neglected in our approach drive SC to zero at a finite doping [20]. We also do not consider the effects of other competing orders (stripes or charge ordering). For large doping, where the pairing $\Delta \to 0$, finite size effects become large because of a growing correlation length. This leads to an overestimate of the range over which SC survives, but it does not qualitatively affect our conclusions [21].

Fermi-surface topology.—Is there a simple way to understand our results? First, we emphasize that the dependence of the phase diagram on the bare dispersion is not controlled by the van Hove singularity in the bare density of states. Even in the particle-hole symmetric case $t' = t'' = 0$, where the van Hove singularity is precisely at the center of the band, the calculated SC order parameter $\Phi(x)$ does not peak at $x = 0$ but rather at an "optimal" doping away from zero. This optimal doping is determined by the interplay between the growth of the pairing amplitude Δ with underdoping and the suppression of phase coherence by strong correlations as $x \to 0$. Irrespective of the values of t' and t'', the renormalized bandwidth is of order

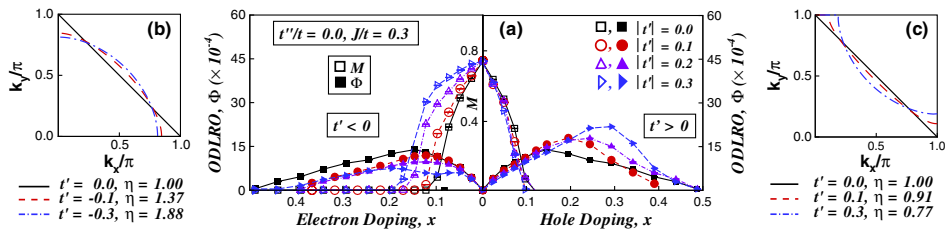

FIG. 1 (color online). (a) Phase diagram of extended t-J model with $t'' = 0$ and t' indicated in the inset, showing Néel magnetization M and the SC order parameter Φ as a function of both hole and electron doping. (b),(c) Shapes of the bare Fermi surface at half filling.

$(xt + J)$, while the scale of the pairing is also of order J. Thus we are not in a weak coupling BCS regime where all the action is in the immediate vicinity of the chemical potential. In fact, the entire band participates in pairing, and the proximity of the van Hove singularity to the chemical potential is not the dominant factor in determining the phase diagram.

We next define a quantity η that characterizes the topology of the Fermi surface at half filling, defined by the bare tight-binding parameters. We show that this single parameter η controls the dependence of the phase diagram on t' and t''. In particular, key features such as the critical doping x_{AFM}, the maximum value of the SC order parameter Φ_{max}, and optimal doping are all determined by η.

For the cases we study, the Fermi surface at half filling can be described as a curve in the first Brillouin zone $k_F(\theta)$ (in polar coordinates) with θ measured from the k_x axis. We define

$$\eta(t'/t, t''/t) = 2[k_F(\pi/4)/k_F(\theta_{\mathrm{min}})]^2, \qquad (3)$$

where θ_{min} is the minimum angle at which a Fermi crossing exists. In the electron-doped case [Fig. 1(b)], $\theta_{\mathrm{min}} = 0$ and $\eta > 1$, corresponding to a convex Fermi surface. In the hole-doped case [Fig. 1(c)], θ_{min} corresponds to the Fermi crossing on the zone boundary leading to a concave Fermi surface with $\eta < 1$. For $t' = t'' = 0$, the particle-hole symmetric case, $\eta = 1$. In Fig. 2 we show the dependence of η on t' and t''. The right panel focuses on the t' dependence of η on the special line $t'' = t'/2$, which corresponds to the parameters obtained by Pavarini *et al.* [5] from electronic structure calculations of single layer cuprates.

In Fig. 3 we show the η dependence of the critical doping x_{AFM} for the vanishing of the AFM order. On the electron-doped side, x_{AFM} increases approximately linearly with η, while for hole doping, x_{AFM} is essentially independent of η. Turning now to superconductivity, we see from Fig. 3 that the SC order parameter Φ_{max} at optimality increases roughly linearly with decreasing η on the hole-doped side. On the electron-doped side, there is a slight linear decrease of Φ_{max} as a function of increasing η. Thus a more concave bare Fermi surface leads to a more stable SC state. We have also studied the dependence of the optimal doping x_{opt} (doping at which Φ attains Φ_{max}) and found a similar correlation with η.

We have thus demonstrated that three characteristics of the phase diagram, x_{AFM}, Φ_{max}, and x_{opt}, are determined by a single parameter η rather than by the details of the bare dispersion. Two systems with a given t and J but with two very different t' and t'' have the same phase diagram provided they correspond to the same value of η. This is clearly illustrated by the specially marked points in Fig. 3 (top left).

To understand how the single parameter η controls the entire phase diagram, we consider the competition between the kinetic and exchange energies. Upon doping the Mott insulator, the carriers attempt to gain kinetic energy (KE). Near half filling, the hopping t between different sublattices disrupts the antiferromagnetic order and increases the exchange energy. On the other hand, the hoppings t' and t'' between the same sublattice do not disturb AFM order and entail no exchange energy penalty. Insight into how the system gains the most KE while keeping the exchange energy increase to a minimum may be obtained from studying the behavior of the KE as a function of doping x.

In Fig. 4(a), we show that the variational Monte Carlo (projected) KE for a convex ($\eta > 1$), a concave ($\eta < 1$), and a half-filled diamond ($\eta = 1$) Fermi surface. In each case the projected KE is closely reproduced by the Gutzwiller approximation [8] result gK_{bare}, where K_{bare} is the bare KE in the unprojected state and $g = 2x/(1 + x)$ is the renormalization factor that takes into account projection.

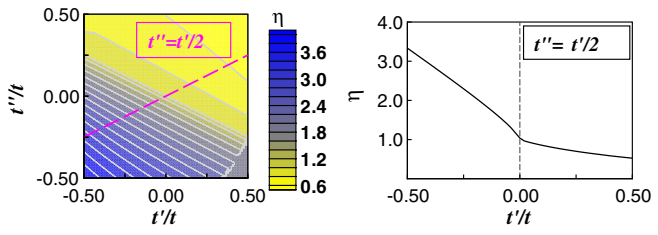

FIG. 2 (color online). Left panel: A contour plot of η as a function of the hopping amplitude t'/t and t''/t. Right panel: Monotonic relationship between η and the range parameter [5] t'/t (for the special case of $t'' = t'/2$).

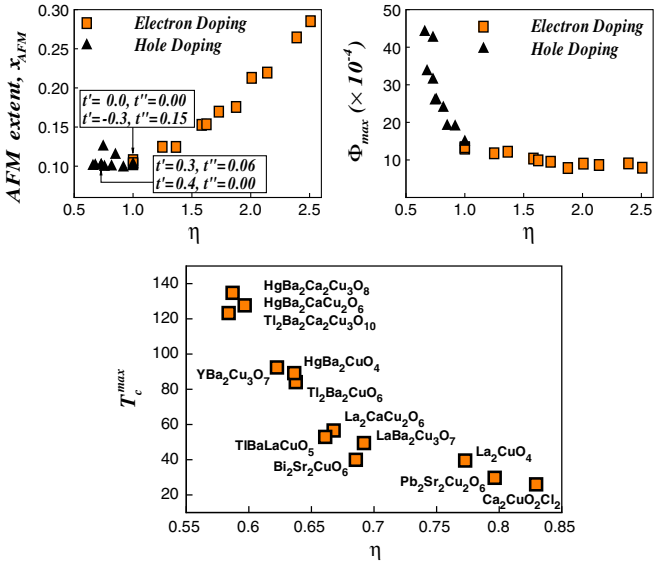

FIG. 3 (color online). Top left panel: The range of doping x_{AFM} of the AFM phase as a function of η. Note that systems with very different bare t's but with the same η have similar x_{AFM}. This is also true for Φ_{max} and optimal doping x_{opt}. Top right panel: SC order at optimal doping Φ_{max} as a function of η. Bottom panel: Correlation between experimental T_c^{max} for hole-doped cuprates and η calculated using tight-binding parameters of Pavarini *et al.* [5].

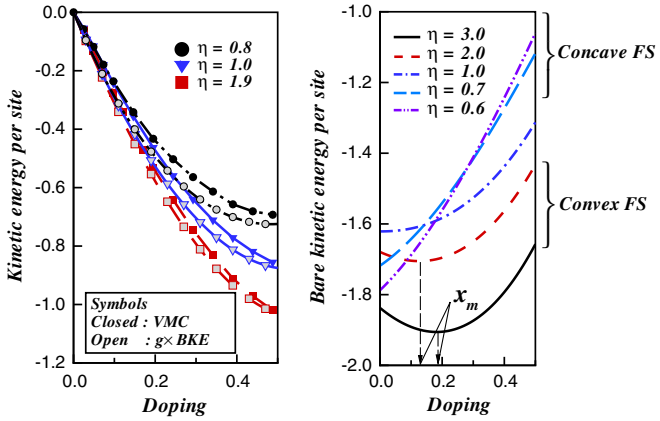

FIG. 4 (color online). Left panel: Comparison of kinetic energy per site obtained from VMC and Gutzwiller projected bare kinetic energy (BKE); $[g = 2x/(1 + x)]$. Right panel: Bare kinetic energy as a function of doping for systems with various η's with different Fermi surface (FS) topologies.

The renormalization factor g is independent of the η parameter, and thus we focus on the bare KE in Fig. 4(b) to understand the η dependence of the competition between KE and superexchange. For electron doping with $\eta > 1$, the bare KE is a nonmonotonic function of doping with a minimum at a finite x_m. Thus up to a doping of x_m, one can gain KE due to t' and t'' without sacrificing exchange energy, thereby stabilizing the AFM state. The doping x_m increases with increasing η [see Fig. 4(b)] which underlies the η dependence of x_{AFM} on the electron-doped side. For the p-h symmetric ($t' = t'' = 0$) case, $\eta = 1$ and the minimum KE is at $x_m = 0$. For hole doping with $\eta < 1$, the bare KE increases monotonically with doping. The exchange energy is best satisfied by means of SC with resonating singlet pairs, while providing for the necessary KE gain, respecting the no-double occupancy constraint. Thus a system with a larger bare KE favors a more stable SC state.

As noted earlier, Pavarini *et al.* [5] suggested an empirical correlation between their range parameter related to t'/t (for the special case of $t'' = |t'|/2$) and $T_c^{\max}$, the maximum T_c within a given cuprate family. We cannot, of course, obtain T_c from our ground state calculation, but the magnitude of the SC order parameter Φ is taken [7,16] as a measure of T_c. We see a strong linear correlation between $\Phi^{\max}$ and η on the hole-doped side in Fig. 3 (top right), suggesting that $T_c^{\max}$ is controlled by η. We corroborate this finding by plotting the experimental $T_c^{\max}$ and the theoretical η (calculated from the tight-binding parameters from Ref. [5]) in the bottom panel of Fig. 3 where excellent correlation between the two is seen. On the electron-doped side, however, we do not predict a strong dependence of $T_c^{\max}$ on the η parameter.

In conclusion, our results provide a unified microscopic picture for the competition between AFM and SC for electron and hole-doped cuprates while also providing insights into a key material parameter η that controls many aspects of the phase diagram, including $T_c^{\max}$. In particular, this work suggests a route to increase $T_c^{\max}$ by creating systems with a small η, i.e., with a highly concave bare Fermi surface at half filling. Even if such band structure engineering may not be easy in solid state materials, it may be possible in optical lattice realizations of strongly correlated Fermions.

We acknowledge support by DST, the India-SERC project/Ramanujan grant (S. P., V. B. S.), NSF-DMR 0706203 (M. R.), and DOE DE-FG02-07ER46423 (N. T.). We thank T. V. Ramakrishnan, H. R. Krishnamurthy, T. Saha-Dasgupta, and R. Sensarma for discussions, and S. Ramaswamy and P. Maiti for computer resources. We also acknowledge the Ohio Supercomputer Center.

[1] J. Orenstein and A. J. Millis, Science **288**, 468 (2000).
[2] Feature article by P. W. Anderson *et al.*, Nature Phys. **2**, 138 (2006).
[3] *Handbook of High-Temperature Superconductivity*, edited by J. R. Schrieffer and J. S. Brooks (Springer, New York, 2007).
[4] P. A. Lee, N. Nagaosa, and X.-G. Wen, Rev. Mod. Phys. **78**, 17 (2006).
[5] E. Pavarini *et al.*, Phys. Rev. Lett. **87**, 047003 (2001).
[6] P. W. Anderson, Science **235**, 1196 (1987).
[7] A. Paramekanti, M. Randeria, and N. Trivedi, Phys. Rev. Lett. **87**, 217002 (2001); Phys. Rev. B **70**, 054504 (2004).
[8] P. W. Anderson *et al.*, J. Phys. Condens. Matter **16**, R755 (2004).
[9] M. Ogata and H. Fukuyama, Rep. Prog. Phys. **71**, 036501 (2008).
[10] G. J. Chen *et al.*, Phys. Rev. B **42**, 2662 (1990).
[11] T. Giamarchi and C. Lhuillier, Phys. Rev. B **43**, 12 943 (1991).
[12] A. Himeda and M. Ogata, Phys. Rev. B **60**, R9935 (1999).
[13] J. C. Campuzano, M. R. Norman, and M. Randeria, in *Superconductivity*, edited by K. H. Bennemann and J. B. Ketterson (Springer-Verlag, Berlin, 2008), Vol. 2, p. 923; A. Damascelli, Z. Hussain, and Z.-X. Shen, Rev. Mod. Phys. **75**, 473 (2003).
[14] O. K. Andersen *et al.*, J. Phys. Chem. Solids **56**, 1573 (1995).
[15] We use the "titled square lattice" with $L^2 + 1$ sites for $L = 9$ with periodic boundary conditions [7].
[16] T. K. Lee and C. T. Shih, Phys. Rev. B **55**, 5983 (1997); T. K. Lee, C.-M. Ho, and N. Nagaosa, Phys. Rev. Lett. **90**, 067001 (2003); C. T. Shih *et al.*, Phys. Rev. Lett. **92**, 227002 (2004).
[17] G. Kotliar *et al.*, Phys. Rev. Lett. **87**, 186401 (2001).
[18] D. Senechal *et al.*, Phys. Rev. Lett. **94**, 156404 (2005).
[19] F. C. Zhang *et al.*, Supercond. Sci. Technol. **1**, 36 (1988).
[20] R. Sensarma and M. Randeria (unpublished).
[21] See diffusion Monte Carlo results of L. Spanu *et al.*, Phys. Rev. B **77**, 024510 (2008), for hole doping.